



Gamma-ray Bursts observed by XMM-Newton

P.T. O'Brien¹, J.N. Reeves², D. Watson³, J. Osborne¹ and R. Willingale¹,

¹ Department of Physics & Astronomy, University of Leicester, University Road, Leicester, LE1 7RH, U.K.

² Laboratory for High Energy Astrophysics, NASA Goddard Space Flight Center, Code 662, Greenbelt, MD 20771, USA

³ Astronomical Observatory, Neils Bohr Institute for Astronomy, Physics and Geophysics, University of Copenhagen, Juliane-Maries, Vej 30, DK-2100, Copenhagen, Denmark

Abstract. Analysis of observations with XMM-Newton have made a significant contribution to the study of Gamma-ray Burst (GRB) X-ray afterglows. The effective area, band-pass and resolution of the EPIC instrument permit the study of a wide variety of spectral features. In particular, strong, time-dependent, soft X-ray emission lines have been discovered in some bursts. The emission mechanism and energy source for these lines pose major problems for the current generation of GRB models. Other GRBs have intrinsic absorption, possibly related to the environment around the progenitor, or possible iron emission lines similar to those seen in GRBs observed with BeppoSAX. Further XMM-Newton observations of GRBs discovered by the Swift satellite should help unlock the origin of the GRB phenomenon over the next few years.

Key words. gamma rays: bursts – supernovae: general – X-rays: general

1. Introduction

Gamma-ray Bursts (GRBs) are thought to signal the birth of a black hole which is for a short period (few to few tens of seconds) fed by a surrounding disk or torus. The progenitor is probably a massive collapsing star, possibly in a binary system, which, as the system collapses, release enormous amounts of energy ($\sim 10^{52}$ erg) which powers a relativistic jet. The jet tunnels its way out of the progenitor star envelope and then interacts with any surrounding material. This interaction results in

an “afterglow” which emits strongly from X-ray to radio wavelengths before fading from view. GRBs can be crudely divided into “short” and “long” bursts depending on the length of the gamma-ray pulse, with the division occurring at about 2 seconds. Virtually all multi-wavelength data, including all that discussed here, has been obtained for long bursts. A recent review of the GRB phenomena is given in Zhang & Meszaros (2004).

Following the discovery of X-ray afterglows, it was soon realised that the X-ray emission provides a probe of the extreme conditions in the GRB jet. The time-dependent X-ray spectrum acts as a monitor of the density, tem-

Send offprint requests to: P.T. O'Brien,
e-mail: pto@star.le.ac.uk

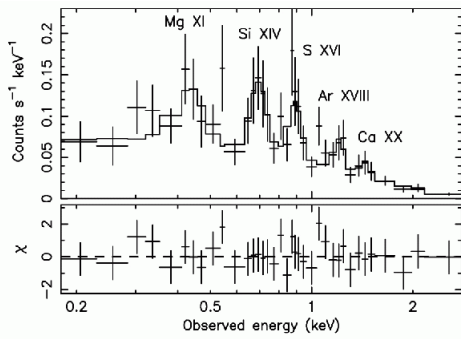


Fig. 1. XMM-Newton EPIC PN spectrum of GRB011211 for the first 5 ksec of the observation (Reeves et al. 2002). Top: count-rate spectrum with best-fit thermal model and Galactic absorption. Bottom: chi-squared fit residuals. The identified emission lines are marked.

perature and emission mechanism, if data of sufficient quality can be obtained. BeppoSAX observations of GRB afterglows revealed emission features usually attributed to iron $K\alpha$ (e.g. Antonelli et al. 2000). The large effective area of the XMM-Newton EPIC instrument affords the opportunity to search for weaker lines, study their time-dependence and to explore the rich, soft X-ray band. Over the last few years XMM-Newton has observed a number of GRBs most of which are described below. Given the operational constraints, XMM-Newton observations have not begun earlier than ~ 0.2 days after the GRB (in the GRB rest-frame), but this is still fast enough for EPIC X-ray spectroscopy of most bursts.

2. GRB observations

The list of GRBs we have analysed is shown in Table 1. GRBs are named in terms of the year+month+day they were detected. A letter is added if several candidates occurred on the same day. The claimed spectral features are listed and discussed below along with the derived “X-ray redshift”. Only two of the GRBs studied have a known optical redshift to date.

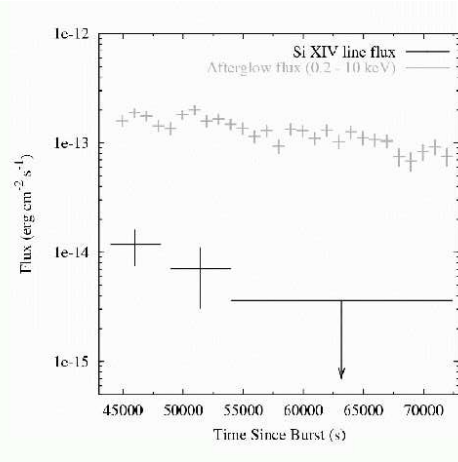


Fig. 2. The decay in the flux of the continuum and the Si XIV line during the XMM-Newton observation of GRB011211. The line is only detected early in the observation.

2.1. GRB011211

GRB011211 was first detected by BeppoSAX at 19:09:21 (UT) on 2001 December 11, and was the longest burst (270 seconds) observed by BeppoSAX. XMM-Newton observations started at 06:16:56 on 2001 December 12, some 11 hours after the gamma-ray flash (Santos-Lleo et al. 2001). The optical redshift of the burst was determined by Holland et al. (2002) to be $z = 2.140 \pm 0.001$, implying an isotropic luminosity of 5×10^{52} erg.

Our analysis of the XMM-Newton data is described in detail in Reeves et al. (2002; 2003). The most important discovery was the serendipitous observation of fading soft X-ray emission lines. These lines are most clearly visible in the first 5 ksec of the observation (Figure 1) and then fade faster than the continuum (Figure 2). The lines are from hydrogenic states of Mg, Si, S, Ar and Ca. Fitted together using Gaussian profiles to represent the lines, a weighted mean X-ray line redshift can be derived of $z = 1.86 \pm 0.07$. This is significantly different from the optical redshift, and implies an outflow velocity of approximately 0.1c.

The presence of decaying, soft X-ray lines was not predicted by GRB models and illus-

Table 1. Summary of the XMM-Newton GRB observations discussed in this paper. ^aRest-frame time interval (in days) over which lines seen. Observing epoch given in brackets if no lines detected. ^bX-ray redshift. ^cOptical redshift. ^dSignificance level for line detection. ^ePublication reference.

GRB	Rest-frame interval ^a	X-ray Lines	z_x^b	z_{opt}^c	Sig. ^d	Ref. ^e
011211	< 0.15 – 0.17	H-like Si, S, Ar	1.86 ± 0.07	2.140	99.97%	1, 2
001025A	< 0.12– > 1.4	(H-like Mg, Si, S)	0.53 ± 0.03		99.87%	3
010220	< 0.31– > 0.56	“Fe”	1.0 ± 0.05		99.84%	3
020322	(0.22 - 0.34)	absorption	1.8(?)			4
030227	0.18– > 0.23	H-like Si, S, He-like Ca	1.39 ± 0.05		99.85%	5
030329	(36.3 and 51.7)	none		0.1685		6, 7

References: 1. Reeves et al. (2002); 2 Reeves et al. (2003); 3. Watson et al. (2002a); 4. Watson et al. (2002b); 5. Watson et al. (2003); 6. Willingale et al. (2004); 7. Tiengo et al. (2003)

trates the potential of XMM-Newton for such work. Equally intriguing is the lack of iron emission in GRB011211. The best-fit model for the emission is, surprisingly, an optically-thin thermal plasma. Although unlikely to be fully physically realistic, this model allows for an estimate of the abundances and ejected mass. For the light elements an abundance some 10 x Solar is required but < 1.4 x Solar for iron. The ejected mass is 4–20 Solar masses.

2.2. GRB030227

Following the discovery of lines in GRB011211 we searched for such features in all GRBs observed by XMM-Newton. The best case, and indeed the strongest of all, is for GRB030227. This GRB was first detected by Integral with the XMM-Newton observation starting some 8 hours after the burst. Watson et al. (2003) discuss the data and show that soft X-ray emission lines are strongly detected near the end of the observation (Figure 3). The lines are rising while the continuum is decaying, although there is a small possible rise in the continuum during in the last ~ 10 ksecs (Figure 4). The X-ray line spectrum in GRB030227 is remarkably similar to that of GRB011211, showing hydrogen and/or helium-like states of Mg, Si, S, Ar and Ca. Again there is no evidence for Fe and neither Co or Ni are detected.

The best-fit redshift derived from the X-ray lines is $z = 1.39^{+0.03}_{-0.06}$. Unfortunately there is,

as yet, no optically determined redshift for this burst so we cannot search for a velocity shift. Nevertheless, the similarity with GRB011211 gives us confidence that a similar phenomena is occurring in both objects. Again, the soft X-ray line spectrum in GRB030227 can be well fitted by a thermal plasma, giving a minimum abundance of 24x Solar for the light elements compared to < 1.6 and < 18 for Fe and Ni respectively. Watson et al. also note that the continuum energy required to produce the X-ray line emission (assuming isotropic emission) is, at the very least, within a factor of 2 of the gamma-ray energy. The time-delayed emergence of bright line emission implies a continuing injection of energy.

The observed spectra of GRB011211 and GRB030227 suggest either little production of heavy elements, in contrast to the usual predictions, or that somehow the heavy elements are missing from the observed ejecta (Watson et al. 2003). The expected abundance patterns depend strongly on the physical conditions, geometry and dynamics of the nucleosynthesis site which could be the progenitor, the disk/torus surrounding the black hole and/or the jet. Disentangling which site dominates will be a major analysis task for the future.

Finally, we note that the presence of soft X-ray lines have been subject to some doubt (e.g. Rutledge & Sako 2003) due to the relatively poor statistics. Although the GRBs are relatively faint, the total number of photons in the XMM-Newton detected X-ray lines are

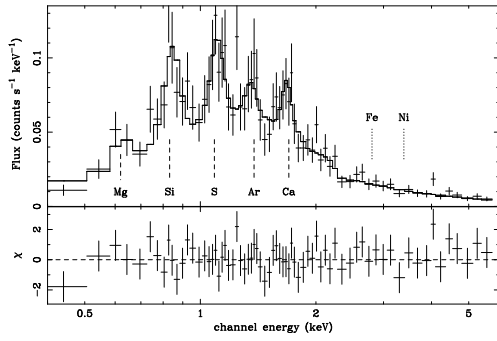


Fig. 3. XMM-Newton EPIC PN spectrum of GRB030227 for the last 11 ksec of the observation (Watson et al. 2003). Top: count-rate spectrum fitted with a powerlaw, Galactic absorption and five Gaussian emission lines. Bottom: chi-squared fit residuals. The identified emission lines are marked at their expected energies for a redshift of $z = 1.39$.

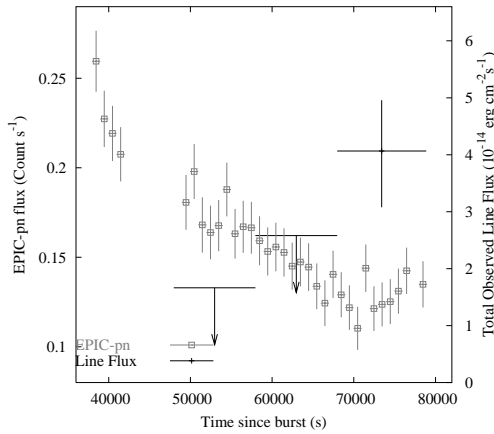


Fig. 4. The light-curve of GRB030227 during the XMM-Newton observation. The continuum ((0.2–10) keV) decays steadily during the observations whereas the emission lines become detectable only at the end.

much higher than in the claimed BeppoSAX features. For example, the claimed iron line in GRB000214 (Antonelli et al. 2000) has ~ 35 photons whereas in GRB011211 there are ~ 115 line photons and ~ 210 in GRB030227. It would therefore seem perverse to accept BeppoSAX detections but not those

from XMM-Newton. More importantly, detailed Monte-Carlo simulations (Reeves et al. 2002; Watson et al. 2003) give a high probability that the observed line features are real. The null probability for GRB011211 is about 4σ whereas for GRB030227 it is 4.4σ .

2.3. GRB001025A

GRB001025A was observed by XMM-Newton some 45 hours after the burst. The XMM-Newton data have poor S/N (Figure 5) but are best fitted by a thermal plasma model providing a redshift of $z = 0.53 \pm 0.03$ (Watson et al. 2002a). No optical redshift exists for this burst.

2.4. GRB010220

GRB010220 was observed by XMM-Newton some 15 hours after the burst. A single powerlaw, with Galactic absorption, provides an acceptable fit but adding a Gaussian emission line at ~ 3.9 keV improves the fit at the 99% level (Figure 6; Watson et al. 2002a). If identified with the iron 6.4 keV $K\alpha$ line, this features gives an X-ray redshift of $z = 1.0 \pm 0.05$. Again no optical redshift has been determined for this burst.

2.5. GRB020322

This burst, discovered by BeppoSAX, shows soft X-ray absorption in excess of that due to the Galaxy (Figure 7; Watson et al. 2002b). Again, no optical redshift has been published, but the best-fit X-ray absorption model, adopting either a neutral or ionised absorber, gives a redshift of $z = 1.8 \pm 1.0$. The best-fit absorbing column at $z = 1.8$ is $1.3 \pm 0.2 \times 10^{22} \text{ cm}^{-2}$. There is no evidence for line emission in these relatively high S/N data.

2.6. GRB030329

The nearby ($z = 0.1685$) GRB030329 is becoming a ‘‘Rosetta Stone’’ object. Its high initial apparent brightness and sky location allowed for intensive, multi-waveband observa-

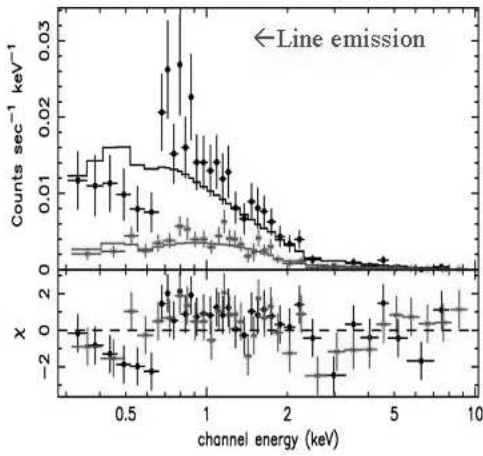


Fig. 5. XMM-Newton EPIC PN and MOS spectra of GRB01025A fitted with a power-law and Galactic absorption. There is an excess emission feature observed at ~ 0.8 keV that can be well fitted with a thermal plasma model (Watson et al. 2002a).

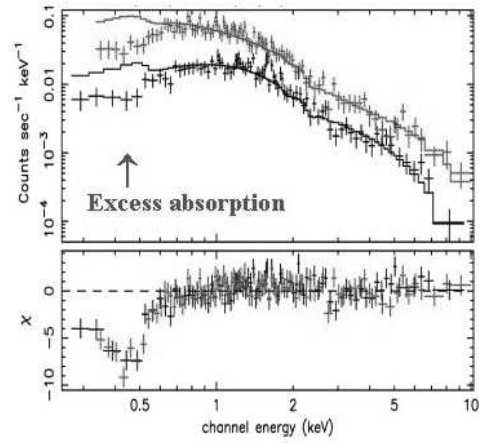


Fig. 7. XMM-Newton EPIC PN and MOS spectra of GRB020322 fitted with a power-law and Galactic absorption. There is an excess absorption feature which can be well fitted with an absorber of redshift $z = 1.8 \pm 1.0$ (Watson et al. 2002b).

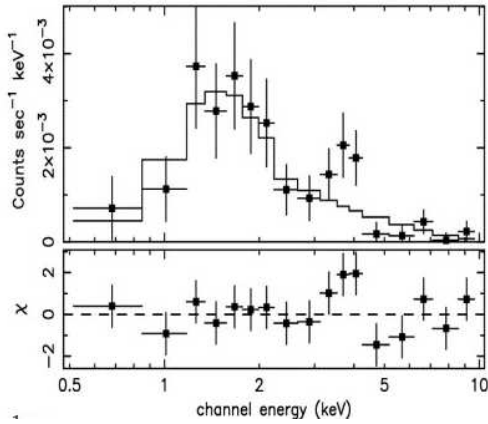


Fig. 6. XMM-Newton EPIC PN spectrum of GRB010220 fitted with a powerlaw and Galactic absorption. The only spectral feature is a possible emission line, which could be due to iron $K\alpha$, at ~ 3.9 keV (Watson et al. 2002a).

tions. Although unable to observe it initially, XMM-Newton has provided invaluable late-time X-ray fluxes (Tiengo et al. 2003) which, when combined with other multi-wavelength data, enabled Willingale et al. (2004) to fit a

fireball shock model to parameterise the temporal behaviour with unprecedented accuracy. The quality of the XMM-Newton spectra provide an accurate measure of both the flux and the shape of the decaying afterglow spectrum 37 and 61 days after the GRB. These spectra provide an important constraint in the modelling.

In Figure 8 we show the evolution of the X-ray and optical spectral indices. For $t < 1$ day the optical and X-ray indices differ by ~ 0.5 demonstrating that the cooling break occurs at $\sim 1.3 \times 10^{16}$ Hz. After a day the X-ray spectral index remains constant while the optical spectrum reddens and is strongly reddened for $t > 10$ days. These changes are coincident with a rapid increase in the optical flux at $t \sim 1$ days relative to the X-ray (Figure 9) which is only partly explained by the concurrent ‘hypernova’ (SN2003dh) seen in the optical (Hjorth et al. 2003). An ‘excess’ flux is also seen in the radio (Willingale et al. 2004). The excess energy implies a longer-duration injection of energy than the initial GRB, possibly due to a longer-lived central engine, an additional broader, slower jet component and/or a super-

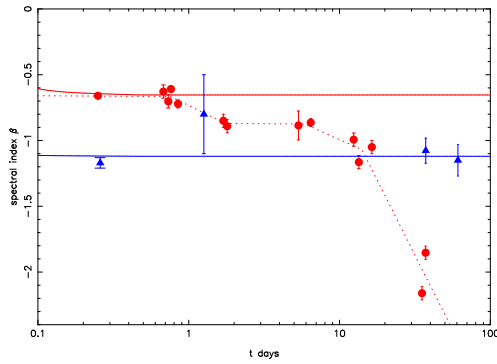


Fig. 8. The observed X-ray (triangles) and optical (circles) spectral indices ($f_\nu \propto \nu^\beta$) as a function of time for GRB030329 (Willingale et al. 2004 and references therein). The dotted line indicates the trend in the optical spectral index. The solid lines show the predicted evolution for the best-fit fireball shock model.

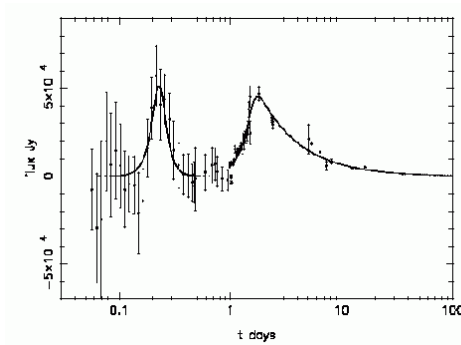


Fig. 9. The residual optical (R band) flux after subtracting the best-fit fireball shock model (Willingale et al. 2004). The curves are simple powerlaw fits for illustration.

nova behaviour unlike others. Whatever the explanation, XMM-Newton is uniquely powerful in allowing a determination of both the X-ray flux and spectral shape at late times.

3. Conclusions

From their discovery in the 1960s, the study of GRBs progressed steadily until the discovery of afterglows. These fixed the distance scale and hence the intrinsic luminosity of the bursts.

The observations of X-ray afterglows have revealed a wealth of spectral detail only just beginning to be understood. XMM-Newton has already made a major contribution to our understanding of GRBs, providing data that challenge and in some cases contradict so-called “standard models”.

Although we have few objects to date, some interesting, possibly related, spectral features are already starting to emerge. For example, the first “optical excess” in GRB030329 occurs at ~ 0.2 days (rest-frame), intriguingly close to the rest-frame interval at which time-dependent, soft X-ray emission-lines are seen in GRB011211 and GRB030227. These events may indicate structure in the jet and/or the surroundings close to the GRB. Obtaining densely-sampled, correlated, multi-wavelength observations of such events is obviously a vital task for the future. This task will be made easier by the launch in 2004 of the dedicated GRB mission, Swift. This mission will discover 2–3 GRBs per week, greatly increasing the number of potential GRB targets for XMM-Newton. We hope XMM-Newton will continue to observe as many GRBs as possible and hence further our understanding.

Acknowledgements. We are grateful for the efforts of the XMM-Newton SOC in carrying out the target of opportunity observations of GRBs.

References

- Antonelli, L.A., et al., 2000, ApJ, 545, L39
- Hjorth, J., et al., 2003, Nature, 423, 847
- Holland, S.T., et al., 2002, AJ, 124, 639
- Reeves, J.N., et al., 2002, Nature, 416, 512
- Reeves, J.N., et al., 2003, A&A, 403, 463
- Rutledge, R.E., Sako, M., 2003, MNRAS, 339, 600
- Santos-Lleo, M., et al., 2001, GRB Coordinates Network Circular 1192
- Tiengo, A., et al., 2003, A&A, 409, 983
- Watson, D., et al., 2002a, A&A, 393, L1
- Watson, D., et al., 2002b, A&A, 395, L41
- Watson, D., et al., 2003, ApJ, 595, L29
- Willingale, R., et al., 2004, MNRAS, in press (astro-ph/0307561)

Zhang, B., Meszaros, P., 2004, International
Journal of Modern Physics A, in press
(astro-ph/0311321)